ALEPH 98-047
CONF 98-021

EPS-HEP99
Abstract 5-411
Parallel session: 5
Plenary session: 5

P R E L I M I N A R Y

Production of D_1 and D_2^* mesons in hadronic Z decays

The ALEPH Collaboration

Abstract

A study of the production of L=1 charmed mesons (D^{**} states) has been performed using four million of Z decays collected by the ALEPH detector at LEP. D_1 ($J^P = 1^+$) state is observed in the decay channel $D^*\pi$, and the D_2^* ($J^P = 2^+$) state in both channels $D^*\pi$, $D\pi$. Since D^{**} states could originate from b hadron decays in $Z \to b\bar{b}$ or from charm fragmentation in $Z \to c\bar{c}$ events, rates are measured separately for $b \to D_1, D_2^*$ and $c \to D_1, D_2^*$. No significant D_2^* production is observed in b hadron decays, while D_2^* production dominates in charm hadronization.

ALEPH contribution to 1999 Summer Conferences
Contact person D. Pallin (dominique.pallin@cern.ch)

1 Introduction

The fragmentation of the charmed quark has been extensively studied through the $D^{*\pm}$ spectrum at LEP [1, 2, 3]. The spin aspect of hadronization, however, is still a poorly known subject, experimentally as well as theoretically. The relative probabilities for producing various spin states in charm hadronization have to be measured. In the hadronization of charm quarks into charmed mesons, mainly $L = 0$ states were supposed to be produced. The first indication for a substantial production of $L = 1$ states in Z decays came from the discrepancy between measured rates of vector and pseudoscalar charm mesons [1, 2, 3] and the expected value from simple spin counting. This question is addressed here where a search for L=1 mesons is presented. This could be studied at LEP in Z decays where D^{**} are produced either directly in the fragmentation of a charm quark in the decays $Z \to c\bar{c}$, or in b hadron decays from $Z \to b\bar{b}$ process.

Four $L = 1$ states of the $c\bar{q}$ system (q = u, d) are predicted, one of total spin 0 ($^3P_0$ in spectroscopic notation) called D_0^*, two spin 1 mass eigenstates ($^1P_1$ and $^3P_1$) called D_1, and one spin 2 called D_2^* ($^3P_2$). Theses states, commonly called D^{**}, are expected to decay via strong interaction into D's and D^{*}'s by emitting a pion. Due to spin-parity conservation in strong decays, the D_1 can decay into $D^*\pi$ only, in a combination of D wave and S wave, whereas the D_2^* can decay into both $D\pi$ and $D^*\pi$ through a D wave only.

In the limit $m_Q \to \infty$, Heavy Quark Effective Theory [4] (HQET) predicts new spin-flavor symmetries for mesons with a heavy quark Q. In the framework of HQET, L=1 charmed mesons are classified in multiplets, according to their light angular momentum j. Two states, one of the D_1 state and the D_2^*, decaying only via a D wave and supposed to be narrow, are grouped in the doublet j=3/2, while the doublet j=1/2 consits of two broad states decaying in S wave, the other D_1 and the D_0^* [5]. In addition, corrections in $1/m_Q$ of HQET allow some mixing between the two D_1 states.

All the narrow states D_1, D_2^* have been observed. Their masses and widths are given in Table 1 [6].

	J^P	Mass (MeV/c^2)	Width (MeV/c^2)	Decay modes
D_1^0	1^+	2422.2 ± 1.8	$18.9^{+4.6}_{-3.5}$	$D^*\pi$
D_2^{*0}	2^+	2458.9 ± 2.0	$23. \pm 5.$	$D\pi$, $D^*\pi$
D_1^+	1^+	$2427. \pm 5.$	$28. \pm 8.$	$D^*\pi$
D_2^{*+}	2^+	$2459. \pm 4.$	$25.^{+8.}_{-7.}$	$D\pi$, $D^*\pi$

Table 1: Masses and widths of the known $L = 1$ non-strange charmed mesons.

A direct search for $Z \to D^{**}X$ decays has already been performed at LEP by ALEPH [7], DELPHI [8] and OPAL [9]. The following study uses the statistics collected by ALEPH between 1991 and 1995, searching for both $D^*\pi$ and $D\pi$ decay mode for the D^{**} states. The D_1^0, D_2^{*0} and D_2^{*+} are fully reconstructed in $D^*\pi$ and $D\pi$ decay

modes [1]:

$$\begin{aligned} D_1^0 &\rightarrow D^{*+}\pi^- \\ D_2^{*0} &\rightarrow D^+\pi^-, D^{*+}\pi^- \\ D_2^{*+} &\rightarrow D^0\pi^+ \end{aligned}$$

An attempt to separate the origin of the D^{**}'s (charm hadronization or b hadron decay) has been made. The higher average momentum of D mesons in $Z \rightarrow c\bar{c}$ than in $b\bar{b}$ and the distance from the primary vertex of the D^{**} vertex are used to select separately D^{**} samples from these two processes.

The purity of $b\bar{b}$ and $c\bar{c}$ samples reaches 95 %, allowing the measurement of the production rates $c \rightarrow D_1, D_2^*$ and $b \rightarrow D_1, D_2^*$.

2 The D Meson Reconstruction

A sample of 4.1 million hadronic Z decays, collected by the ALEPH detector [10] at LEP, has been selected as described in [7]. Tracks in each event are grouped in two hemispheres according to the event thrust axis. D mesons candidates are searched for in each hemisphere from track combinations with relevant mass hypotheses. The D^0 and D^+ are fully reconstructed in the modes $D^0 \rightarrow K^-\pi^+$, $D^0 \rightarrow K^-\pi^+\pi^-\pi^+$, $D^0 \rightarrow K^-\pi^+\pi^0$ and $D^+ \rightarrow K^-\pi^+\pi^+$. Once a D^0 candidate is found, a pairing with an additional low momentum track (referred to as π_s^+) is made to reconstruct a D^{*+} through its decay mode $D^0\pi^+$.

The combinatorial background increases with the number of tracks issued from the D meson decay, and lies mainly at low D meson momentum. Selection criteria reduce a large fraction of this background. The main characteristics of the D^0, D^+ and D^{*+} selections (see [11] for details) are summarized hereafter. The invariant mass of a system combining 2 tracks ($D^0 \rightarrow K^-\pi^+$), 3 tracks ($D^0 \rightarrow K^-\pi^+\pi^0$, $D^+ \rightarrow K^-\pi^+\pi^+$) or 4 tracks ($D^0 \rightarrow K^-\pi^+\pi^-\pi^+$) with relevant mass assignment is required to be within two standard deviations of the D^0 (D^+) mass. A low momentum pion ($P_{\pi_s^+} < 4.2$ GeV/c) is added to the D^0 system of 2, 3 or 4 tracks and a D^{*+} candidate is kept if the mass difference $\Delta M \equiv M(\pi_s^+ D^0) - M(D^0)$ lies between 143.5 MeV/c^2 and 147.5 MeV/c^2.

Then, the combinatorial background is reduced by exploiting the scalar nature of the D^0 and D^+, and identifying kaon particles using dE/dx measurement in the TPC. A cut $|\cos\theta^*| < 0.8$ is performed where θ^* is the angle between the sphericity axis of the $D^{0/+}$ system and the $D^{0/+}$ direction in the $D^{0/+}$ rest frame. The kaon track candidate, which must have a momentum greater than 2.5 GeV/c, is required to have a dE/dx measurement closer to the expectation for a kaon than for a pion. When necessary, to further reduce the background contribution, D^0 and D^+ candidates are selected if associated tracks form a common vertex and if this vertex is not consistent with the main vertex.

[1] The charge conjugate states are implicitely considered.

3 The b/c Separation

The c $\rightarrow$ D and b $\rightarrow$ D contributions [2] are separated, thanks to their differences in D energy spectrum, and exploiting the separation existing between the main vertex and the b hadron decay vertex due to b lifetime. The average fraction of the beam energy carried by a D meson in a Z $\rightarrow$ c$\bar{\text{c}}$ event is $< X_E^{\text{D}} >_{\text{c}} \simeq 0.5$ while in a Z $\rightarrow$ b$\bar{\text{b}}$ event, this value is reduced to $< X_E >_{\text{b}} \simeq 0.3$, the W taking a part of b hadron energy in the decay B $\rightarrow$ WD.

If the D originates from the Z $\rightarrow$ c$\bar{\text{c}}$ process, the tracks which belong to the D hemisphere should come from the primary vertex, except the tracks from the D^0 or D^+ decay. On the other hand, in a decay b $\rightarrow$ DX, some tracks are issued from the b hadron decay vertex, and the measurement of their impact parameter [12] should reflect the large b hadron lifetime. The probability p_t that a track was coming from the primary vertex is calculated for all these tracks except for the tracks assigned to the D^0 or D^+ particle. A D^{*+} meson candidate will be classified c $\rightarrow$ D^{*+} if the D^{*+} meson fractional energy is greater than 0.5 and if each track in the D^{*+} hemisphere, except D^0 decay products, are consistent with originating from the primary vertex with a probability greater than 5%. For the c $\rightarrow$ D^0 and c $\rightarrow$ D^+ samples, only a fractional energy greater than 0.55 is required because this cut has the same effect than the track probability cut for reducing b contribution, and removes in addition a part of the large remaining background.

The b $\rightarrow$ D sample is formed with candidates for which a least one track, except D decay products, is not consistent with originating from the primary vertex. A slight cut on the $\text{D}^{(*)}$ meson fractional energy ($X_E^{\text{D}^{(*)}}$ greater than 0.25) is performed, in order to reduce the huge combinatorial background lying at low X_E. To further enhance the purity in b $\rightarrow$ D process, cuts on the decay length significance are performed on D^0 and D^+ candidates.

4 The D Meson Samples

4.1 The c $\rightarrow$ D^* Sample

The invariant mass distributions in the charm enriched sample for $\text{D}^{*+} \rightarrow \text{D}^0\pi_s^+$ channels are shown in figure 1(a). The D^{*+} signals are extracted from these distributions. The shape of the combinatorial background contributions are taken from the Monte Carlo simulation, and their size under the peak are evaluated by fitting the spectra outside the signal region. For $\text{D}^0 \rightarrow \text{K}^-\pi^+\pi^-\pi^+$ and $\text{D}^0 \rightarrow \text{K}^-\pi^+\pi^0$ channel, the signal extraction is more complicated due to the presence of a tail induced by partially reconstruced D^0 mesons. For theses channels the total signal shape is taken from the Monte Carlo simulation and its size under the mass window is extracted by a fit to the data using both contribution, background and signal. The final sample consist of 10199 ± 121 D^{*+}.

The charm purity in this sample, f_c, is measured on data by applying a lifetime-mass tag [12] on the hemisphere opposite to the D^{*+} meson. This tag selects b hemispheres with a 99% purity, and the fraction, $f_{\text{b-tag}}$, of D^{*+} mesons that survive the b-tag cut is used to extract the charm fraction $f_{\text{c}} = \frac{\epsilon_{\text{b}\bar{\text{b}}} - f_{\text{b-tag}}}{\epsilon_{\text{b}\bar{\text{b}}} - \epsilon_{\text{c}\bar{\text{c}}}}$, where $\epsilon_{\text{b}\bar{\text{b}}}$ and $\epsilon_{\text{c}\bar{\text{c}}}$ are the b-tag

[2] hereafter D stands for D^0, D^+ or D^{*+}

efficiency respectively for b events measured from an unbiased $Z \to b\bar{b}$ data sample, and charm events taken from Monte Carlo simulation [11] [12].

4.2 The $b \to D^*$ Sample

The b sample has a higher background contribution from low momentum fake D^*'s. A common vertex is required for the tracks associated to the decays $D^0 \to K^-\pi^+$ and $D^0 \to K^-\pi^+\pi^+\pi^-$ with a projected decay length greater than unity ($D^0 \to K^-\pi^+$ case) or greater than three ($D^0 \to K^-\pi^+\pi^+\pi^-$ case). For the $D^0 \to K^-\pi^+\pi^0$ channel, no vertexing cuts are required due to the presence of a neutral track in the decay products. Instead, the background is reduced by taking into account underlying resonances (mainly $D^0 \to K^-\rho^+$) contributing to this decay channel. $D^0 \to K^-\pi^+\pi^0$ candidates are selected if the $(K^-\pi^+)$ and $(K^-\pi^0)$ invariant masses are in the windows $0.65 GeV/c^2 < M(K^-\pi^+) < 1.1 GeV/c^2$ and $1.5 GeV/c^2 < M(K^-\pi^0) < 1.675 GeV/c^2$; or $1.5 GeV/c^2 < M(K^-\pi^+) < 1.675 GeV/c^2$ and $0.6 GeV/c^2 < M(K^-\pi^0) < 1.2 GeV/c^2$. The invariant mass distributions in the b enriched sample for $D^{*+} \to D^0\pi_s^+$ channels are shown in figure 2(a). The D^{*+} signals and b purity are extracted from these distributions following the same procedure as for the charm sample. The final sample consists of 8982 ± 112 D^{*+} enriched in D^{*+} originating from a b hadron decay .

4.3 The $c \to D$ Sample

The $c \to D^0, D^+$ sample suffers from an important combinatorial background, since in the D^* samples, the reduction of the combinatorial background was mainly obtained thanks to the small Q value existing in the $D^{*+} \to D^0\pi_s^+$ decay. For this reason, the channel $D^0 \to K^-\pi^+\pi^0$ is not used in this selection. In addition to a vertexing requirement, the cut on the D fractionnal energy is raised to $X_E^D > .55$. The resulting invariant mass distributions are shown in figure 1(b)(c). The fractions of combinatorial background events are estimated from the mass distributions. The samples contain 15206 ± 357 D^0 and 6040 ± 157 D^+ enriched in charmed mesons originating from the hadronization of a charm quark.

4.4 The $b \to D$ Sample

Only the gold-plated decay channel $D^0 \to K^-\pi^+$ is considered here. To fight the huge background and to further enrich in b events, the cut on the projected decay significance is raised to three standard deviations. After background subtraction, 8603 ± 133 D^0 are found in the selection window of the mass distribution(figure 2(b)).

5 Search for $D^{**} \to D^*\pi$

A search is performed for decays of the D_1^0 and D_2^{*0} into $D^{*+}\pi^-$. D^{*+} candidates selected as described above are paired with another charged track assumed to be a pion (referred to as π_{**}). Then a search is performed for a common vertex for the D^0, the soft π and the π_{**} tracks.

5.1 $c \rightarrow D^{**}$

The charm sample is selected by requiring a D^{**} vertex consistent with coming from the main vertex within three standard deviations of the decay length resolution. The main combinatorial background arises from fragmentation tracks associated to a D^{*+} meson. The cosine of the angle θ_{**} between the π_{**} and the D^{**} flight direction in the D^{**} rest frame peaks at -1 for this contribution which is reduced by requiring $\cos\theta_{**} > -0.9$. The final mass difference distribution $\Delta M^{**} \equiv M(D^{*+}\pi^-) - M(D^{*+})$ for $(D^{*+}\pi^-)$ combinations is shown in figure 3(a) in which the fraction of mesons originating from the hadronization of a charm quark is 94%.

5.2 $b \rightarrow D^{**}$

The b sample is selected by requiring a D^{**} vertex displaced from the primary vertex by at least two standard deviations of the decay length resolution. No cut is performed on the $\cos\theta_{**}$ distribution since the contribution from fragmentation track is here less important due to the fact that the π_{**} track must come from a secondary vertex. The final ΔM^{**} distribution in the b sample is shown in figure 6(a) in which the fraction of mesons originating from b decays is 92%.

5.3 Fitting Procedure and Results

The experimental resolution on ΔM^{**} is estimated to be 4 MeV/c^2 from a Monte Carlo simulation whereas the natural widths of the resonances have been measured to be about 20 to 25 MeV/c^2 (see table 1). Enhancements in the mass distributions 3(a) and 6(a) are observed at expected D_1 and D_2^* masses. There is no visible contribution from broad states. Thus, an unbinned maximum likelihood fit to these distributions is performed using the sum of two Breit Wigner functions (corresponding to D_2^{*0} and D_1^0) for the signal and the following three parameters function to parameterise the background.

$$\frac{dN}{d(\Delta M^{**})} = a(\Delta M^{**} - m_\pi)^b exp(-c(\Delta M^{**} - m_\pi))$$

The background shape is given by the form of the distribution of the wrong sign combination $(D^{*+}\pi^+)$ obtained from the data in b and c samples (Figures 3 and 6 (b)). The masses and widths are fixed to the measurements given in table 1, the widths being increased by 2 MeV/c^2 to account for the experimental resolution.

The fitted numbers of events in the peaks are given in table 2 for the charm sample and in table 4 for the b sample. The ratio of the two Breit Wigner contributions for D^{**0} produced in charm hadronization is

$$\frac{N_{D_2^{*0}}}{N_{D_2^{*0}} + N_{D_1^0}} = (53 \pm 7_{stat} \pm 6_{syst})\%,$$

while a lower limit of

$$\frac{N_{D_2^{*0}}}{N_{D_2^{*0}} + N_{D_1^0}} < 20\% \quad at \quad 95\% CL$$

is found for D^{**0} produced in b decays.

The efficiency, ε_{**}, to reconstruct a D^{**0} once a D^{*+} is selected is obtained from Monte-Carlo simulation. Nevertheless, in case of partial alignment of the D^{**} with respect with the boost axis, the efficiency of the $\cos\theta_{**}$ cut is not well determined in the Monte Carlo, the simulation containing an isotropic decay of the D^{**}. This D^{**} angular distribution, of the form $1 + \alpha\cos^2\theta_{**}$, was extracted from the data in the charm sample. The total efficiencies are reported in table 3 for the charm selection and in table 5 for the b selection.

6 Search for $D^{**} \to D\pi$

As the D is more frequently produced than the D^* in D_2^* decays, it is appropriate to look for D^{**} decays in $D\pi$. The selection follows the same procedure as for the $D^{**} \to D^*\pi$ selection, adding a charged track assumed to be pion to the D candidate, and looking for a common vertex for the combination.

6.1 $c \to D^{**}$

In the charm sample, the D^{**} vertex is required to come from the main vertex as in section 5. Again, the contribution from fragmentation tracks is reduced by a cut on the $\cos\theta_{**}$ distribution. In addition, events with $(D^0\pi^+)$ systems compatible with coming from a $D^{*+} \to D^0\pi_s^+$ decay are removed. The final mass difference distribution $\Delta M^{**} \equiv M(D\pi) - M(D)$ for $(D^0\pi^+)$ combinations is shown in figure 4(a) and in figure 5(a) for $(D^+\pi^-)$ combinations. In these samples, the fraction of mesons originating from the hadronization of a charm quark is 90%.

6.2 $b \to D^{**}$

$(D\pi)$ combinations in the b sample are also selected in the same way as in section 4 with a rejection of events where a $(D^0\pi^+)$ combination is found to beconsistent with a $D^{*+} \to D^0\pi_s^+$ decay. The final mass difference distribution $\Delta M^{**} \equiv M(D\pi) - M(D)$ for $(D^0\pi^+)$ combinations is shown in figure 7(a), in which the fraction of mesons originating from a b decay is 96%.

6.3 Fitting Procedure and Results

The right-sign distributions are fitted to a background function, a Breit Wigner representing the production of the D_2^* and two other Breit Wigner functions taking into account satellite peaks. In the $(D^0\pi^+)$ samples the satellite peaks arise from the decays $D^{**+} \to D^{*0}\pi^+, D^{*0} \to D^0\pi^0/\gamma$, where the π^0/γ is missing, and from $D^{**0} \to D^{*+}\pi^-, D^{*+} \to D^+\pi^0/\gamma$ in the $(D^+\pi^-)$ sample. The corresponding production rates for the D_1 and D_2^* are derived from the results of section 4 and weighted by the relative efficiency on the satellite peak over the signal peak deduced from a Monte Carlo simulation. The fitted numbers of events in the peaks are given in table 6 for the charm sample and in table 8 for the b sample. In the charm sample, the D^{**} angular distribution was extracted from data assuming the form $1 + \alpha\cos^2\theta_{**}$. The overall efficiencies are reported in table 7 for the charm selection and in table 9 for the b selection.

7 Production Rates

The production rates are extracted from reconstruction efficiencies, branching fractions [3] and the measured numbers of D_1 and D_2^* in the samples. In charm hadronization, the production rates are found to be :

$$\frac{\Gamma(Z \to c/\bar{c} \to D_1^0/\overline{D}_1^0 X)}{\Gamma_{Had}} B(D_1^0 \to D^{*+}\pi^-) = (0.37 \pm 0.075_{stat} \pm 0.06_{syst})\%$$

$$\frac{\Gamma(Z \to c/\bar{c} \to D_2^{*0}/\overline{D}_2^{*0} X)}{\Gamma_{Had}} B(D_2^{*0} \to D^{*+}\pi^-) = (0.41 \pm 0.075_{stat} \pm 0.07_{syst})\%$$

$$\frac{\Gamma(Z \to c/\bar{c} \to D_2^{*0}/\overline{D}_2^{*0} X)}{\Gamma_{Had}} B(D_2^{*0} \to D^{+}\pi^-) = (0.64 \pm 0.15_{stat} \pm 0.11_{syst})\%$$

$$\frac{\Gamma(Z \to c/\bar{c} \to D_2^{*+}/D_2^{*-} X)}{\Gamma_{Had}} B(D_2^{*+} \to D^{0}\pi^+) = (0.71 \pm 0.16_{stat} \pm 0.13_{syst})\%$$

Assuming that the two charge states are produced at the same rate, an average of the last two measurements leads to

$$\frac{\Gamma(Z \to c/\bar{c} \to D_2^*/\overline{D}_2^* X)}{\Gamma_{Had}} B(D_2^* \to D\pi) = (0.68 \pm 0.11_{stat} \pm 0.10_{syst})\%,$$

which used together with the second measurement gives a measurement of the ratio:

$$\frac{B(D_2^* \to D\pi)}{B(D_2^* \to D^*\pi)} = 1.6 \pm 0.4_{stat} \pm 0.3_{syst}$$

in agreement with the world average of 2.3 ± 0.6 [6], while the prediction is about 2.5 [13].

Taking into account the isospin factor of the D^{**} decays, and assuming that only $D^*\pi$ and $D\pi$ decay modes occur, the fractions of D_1 and D_2^* produced in charm hadronization is found to be :

$$c \to D_1 = (3.2 \pm 0.9)\% \qquad c \to D_2^* = (9.4 \pm 1.9)\%$$

These measurements are in agreement with OPAL: $c \to D_1 = (4.2 \pm 1.5)\%$ and $c \to D_2^* = (10.4 \pm 5.0)\%$. They can be compared with the theoretical prediction of $c \to D_1 = 3.5\%$, $c \to D_2^* = 4.7\%$ from [14] based on thermodynamical assumptions to derive hadron abundances in e^+e^- collisions, or with the prediction from [15] $c \to D_1, D_2^* = 17.0\%$ using a simple formulation within string fragmentation to describe the LEP data. A simple spin counting argument leads to $\frac{c \to D_1}{c \to D_2^*} = 3/5 = 0.6$ which is higher than the measured ratio of 0.34 ± 0.12. D^{**} production only has a small influence on the ratio $P_V = V/V + P$, measuring the relative probability to produce a charmed vector state among all charmed vector and pseudoscalar states. Indeed, this ratio is measured to be $P_V^{**} = 0.55 \pm 0.07$ for D and D^* originating form D^{**} whereas the inclusive measurement including all sources of D and D^* leads to a value $P_V = 0.595 \pm 0.045$ [1], very close to P_V^{**}.

[3] The used branching fractions are: $B(D^{*+} \to D^0\pi_s^+) = 0.683 \pm 0.014$, $B(D^0 \to K^-\pi^+) = .0383 \pm 0.0012$, $B(D^0 \to K^-\pi^+\pi^-\pi^+) = 0.075 \pm 0.004$, $B(D^0 \to K^-\pi^+\pi^0) = 0.139 \pm 0.009$ and $B(D^+ \to K^-\pi^+\pi^+) = 0.091 \pm .006$.

In b hadron decays, the production rates of D^{**} are deduced to be:

$$\begin{aligned}
\frac{\Gamma(Z \to b/\bar{b} \to D_1^0/\overline{D}_1^0 X)}{\Gamma_{Had}} B(D_1^0 \to D^{*+}\pi^-) &= (0.66 \pm 0.16_{stat} \pm 0.12_{syst})\% \\
\frac{\Gamma(Z \to b/\bar{b} \to D_2^{*0}/\overline{D}_2^{*0} X)}{\Gamma_{Had}} B(D_2^{*0} \to D^{*+}\pi^-) &< 0.13\% \quad (95\%\ C.L.) \\
\frac{\Gamma(Z \to b/\bar{b} \to D_2^{*+}/\overline{D}_2^{*+} X)}{\Gamma_{Had}} B(D_2^{*+} \to D^0\pi^+) &< 0.55\% \quad (95\%\ C.L.)
\end{aligned}$$

These measurements lead to:

$$b \to D_1 = (4.6 \pm 1.4)\% \qquad b \to D_2^* < 3.9\% \quad (95\%\ C.L.)$$

where the two last results are summed assuming that the two channels $D\pi$ and $D^*\pi$ saturate the D_2^* decay, the statistical and systematical errors being added in quadrature to set the upper limit. These measurements are consistent with previous investigations of D^{**} production in semileptonic b decays [16, 17], where the D_2^* state production is suppressed with respect to the D_1 production rate. Predictions on $\frac{b \to D_1 l\nu}{b \to D_2^* l\nu}$ made for semileptonic b decay into D^{**} should be also valid for hadronic two-body decay $B \to D^{**}\pi$. A recent prediction [18] $\frac{b \to D_2^* l\nu}{b \to D_1 l\nu} = 1.55 \pm 0.15$ seems to be disfavoured by these measurements and other measurements in the semileptonic sector [16, 17]. This could be an indication that the infinite mass limit in HQET is only approximate and order $\Lambda_{QCD}/m_{c,b}$ corrections have to be taken into account [19].

8 Conclusion

A significant production of $L = 1$ charmed mesons (D_1 and D_2^* states) has been observed. In charm hadronization, both D_1 and D_2^* states are produced with production rates :

$$c \to D_1 = (3.2 \pm 0.9)\% \qquad c \to D_2^* = (9.4 \pm 1.9)\%,$$

while in b decays, only the D_1 state is clearly seen:

$$b \to D_1 = (4.6 \pm 1.4)\% \qquad b \to D_2^* < 3.9\% \quad (95\%\ C.L.)$$

For the D_2^* state, the ratio of branching fraction into $D\pi$ over $D^*\pi$ is found to be:

$$\frac{B(D_2^* \to D\pi)}{B(D_2^* \to D^*\pi)} = 1.6 \pm 0.4_{stat} \pm 0.3_{syst}$$

in agreement with the world average of 2.3 ± 0.6 [6].

Since the two mechanisms for producing D^{**} are distinct in $Z \to c\bar{c}$ and $Z \to b\bar{b}$, the relative production rate of the spin 2 state (D_2^*) with respect to the spin 1 state (D_1) could be different. Indeed, no significant D_2^* production is observed in b hadron decays, while D_2^* production dominates in charm hadronization.

c	$\mathbf{D_1^0}$	$\mathbf{D_2^{*0}}$
$\mathbf{N_{D^{**}0}}$	$\mathbf{216 \pm 40_{stat} \pm 30_{syst}}$	$\mathbf{219 \pm 40_{stat} \pm 37_{syst}}$

Table 2: *Charm sample,* $c \to D^{**0}X, D^{**0} \to D^{*+}\pi^-_{**}$*: Fitted numbers of* D_1^0 *and* D_2^{*0} *in the* ΔM^{**} *distributions. Systematic uncertainties on these numbers arise from uncertainties on the widths and masses of the* D^{**}*, the combinatorial background parameterisation and the remaining* $b \to D^{**}$ *contribution.*

	$\mathbf{D^{**0} \to \pi^-_{**}[\pi^+_S(K^-\pi^+)]}$ (%)	$\mathbf{D^{**0} \to \pi^-_{**}[\pi^+_S(K^-\pi^+\pi^0)]}$ (%)	$\mathbf{D^{**0} \to \pi^-_{**}[\pi^+_S(K^-\pi^+\pi^-\pi^+)]}$ (%)
$\varepsilon_{\mathbf{c \to D^{**}}}$	$\mathbf{16.3 \pm 1.3}$	$\mathbf{3.8 \pm 0.5}$	$\mathbf{10.1 \pm 1.2}$
$\varepsilon_{\mathbf{b \to D^{**}}}$	$\mathbf{0.7 \pm 0.1}$	$\mathbf{0.2 \pm 0.1}$	$\mathbf{0.6 \pm 0.1}$

Table 3: *Charm sample,* $c \to D^{**0}X, D^{**0} \to D^{*+}\pi^-_{**}$*: Overall efficiency of the selection in each decay channel.* $\varepsilon_{\mathbf{c \to D^{**}}}$ *is for* D^{**} *originating from a c quark, and* $\varepsilon_{\mathbf{b \to D^{**}}}$ *for* D^{**} *produced in b decays.*

b	$\mathbf{D_1^0}$	$\mathbf{D_2^{*0}}$
$\mathbf{N_{D^{**}0}}$	$\mathbf{253 \pm 57_{stat} \pm 41_{syst}}$	$\mathbf{-11 \pm 34_{stat} \pm 11_{syst}}$

Table 4: *b sample,* $b \to D^{**0}X, D^{**0} \to D^{*+}\pi^-_{**}$*: Fitted numbers of* D_1^0 *and* D_2^{*0} *in the* ΔM^{**} *distributions. Systematic uncertainties on these numbers arise from uncertainties on the widths and masses of the* D^{**}*, the combinatorial background parameterisation and the remaining* $c \to D^{**}$ *contribution.*

	$\mathbf{D^{**0}\to\pi^-_{**}[\pi^+_S(K^-\pi^+)]}$ (%)	$\mathbf{D^{**0}\to\pi^-_{**}[\pi^+_S(K^-\pi^+\pi^0)]}$ (%)	$\mathbf{D^{**0}\to\pi^-_{**}[\pi^+_S(K^-\pi^+\pi^-\pi^+)]}$ (%)
$\varepsilon_{\mathbf{b\to D^{**}}}$	$\mathbf{13.0\pm1.2}$	$\mathbf{2.2\pm0.2}$	$\mathbf{6.3\pm0.7}$
$\varepsilon_{\mathbf{c\to D^{**}}}$	$\mathbf{1.8\pm0.5}$	$\mathbf{0.2\pm0.1}$	$\mathbf{0.6\pm0.2}$

Table 5: *b sample,* $b\to D^{**0}X, D^{**0}\to D^{*+}\pi^-_{**}$*: Overall efficiency of the selection in each decay channel.* $\varepsilon_{\mathbf{c\to D^{**}}}$ *is for* D^{**} *originating from a c quark, and* $\varepsilon_{\mathbf{b\to D^{**}}}$ *for* D^{**} *produced in b decays.*

c	$\mathbf{N_{D^*_2}}$
$\mathbf{D^{*+}_2}$	$\mathbf{159\pm35_{stat}\pm24_{syst}}$
$\mathbf{D^{*0}_2}$	$\mathbf{118\pm28_{stat}\pm14_{syst}}$

Table 6: *Charm sample,* $c\to D^{**}X, D^{**}\to D\pi_{**}$*: Fitted numbers of* $D_2^{*0/+}$ *in the* ΔM^{**} *distributions. Systematic uncertainties on these numbers arise from uncertainties on the widths and masses of the* D^{**}*, the combinatorial background parameterisation and the remaining* $b\to D^{**}$ *contribution.*

	$\mathbf{D^{*+}_2\to\pi^+_{**}(K^-\pi^+)}$ (%)	$\mathbf{D^{*+}_2\to\pi^+_{**}(K^-\pi^+\pi^-\pi^+)}$ (%)	$\mathbf{D^{*0}_2\to\pi^-_{**}(K^-\pi^+\pi^+)}$ (%)
$\varepsilon_{\mathbf{c\to D^{**}}}$	$\mathbf{7.2\pm0.7}$	$\mathbf{3.5\pm0.5}$	$\mathbf{4.9\pm0.5}$
$\varepsilon_{\mathbf{b\to D^{**}}}$	$\mathbf{0.5\pm0.2}$	$\mathbf{0.5\pm0.1}$	$\mathbf{0.4\pm0.1}$

Table 7: *c sample,* $c\to D^{**}X, D^{**}\to D\pi_{**}$*: Overall efficiency of the selection in each decay channel.* $\varepsilon_{\mathbf{c\to D^{**}}}$ *is for* D^{**} *originating from a c quark, and* $\varepsilon_{\mathbf{b\to D^{**}}}$ *for* D^{**} *produced in b decays.*

b	$\mathbf{N_{D^*_2}}$
$\mathbf{D^{*+}_2}$	$\mathbf{21\pm29_{stat}\pm14_{syst}}$

Table 8: *b sample,* $b\to D^{**}X, D^{**}\to D\pi_{**}$*: Fitted number of* D_2^{*+} *in the* ΔM^{**} *distribution. Systematic uncertainties on these number arise from uncertainties on the widths and masses of the* D^{**}*, the combinatorial background parameterisation and the remaining* $c\to D^{**}$ *contribution.*

	$\mathbf{D_2^{*+} \to \pi^+_{**}(K^-\pi^+)}$ (%)
$\varepsilon_{\mathbf{b \to D^{**}}}$	$\mathbf{8.0 \pm 0.8}$
$\varepsilon_{\mathbf{c \to D^{**}}}$	$\mathbf{0.4 \pm 0.2}$

Table 9: *b sample,* $b \to D^{**}X, D^{**} \to D\pi_{**}$*: Overall efficiency of the selection in each decay channel.* $\varepsilon_{\mathbf{c \to D^{**}}}$ *is for* D^{**} *originating from a c quark, and* $\varepsilon_{\mathbf{b \to D^{**}}}$ *for* D^{**} *produced in b decays.*

References

[1] ALEPH Collaboration, *Study of Charm Production in Z Decays*, Contribution number 983 to this conference (Vancouver 1998).

[2] OPAL Collaboration, *Determination of the Production Rate of D^{*0} Mesons and of the Ratio V/(V+P) in $Z \to c\bar{c}$ Decays* and reference therein, CERN-EP/98-06, to appear in Eur. Phys. J. C.
OPAL Collaboration, Z. Phys. **C67**, (1995) 27

[3] DELPHI Collaboration, *Study of Charm Mesons Production in Z Decays and Measurement of* Γ_c/Γ_h, Contribution to EPS-HEP Conference (Brussels), eps0557 (1995).
DELPHI Collaboration, *Study of Exclusive D^{*+} Production in Z^0 Decays*, contribution to IHEP Conference (Warsaw), PA01-058 (1996)

[4] N Isgur and M Wise, Phys. Lett. **B232**, (1989) 113
M. Neubert, Phys. Reports **A245** (1994) 259

[5] N Isgur and M Wise, Phys. Rev. Lett. **66**, (1991) 1130
J. L. Rosner, Comm. Nucl.Part.Phys. 16 (1986) 109.

[6] Particle Data Group, Phys. Rev. **D54** (1996) 1.

[7] ALEPH Collaboration, *Production of Charmed Meson in Z Decays*, Z. Phys. **C62** (1994) 1.
ALEPH Collaboration, *Production of Orbitally Excited Charmed Mesons in $Z \to c\bar{c}$ Decays*, contribution to IHEP Conference (Warsaw), PA01-075 (1996)

[8] DELPHI Collaboration, *First Evidence for a Charm Radial Excitation, $D^{*'}$*, CERN-PPE/98-030, to appear in Phys. Lett. B.

[9] OPAL Collaboration, *Production of P-Wave Charm and Charm-strange Mesons in Hadronic Z^0 Decays*, CERN-PPE/97-035, to appear in Z. Phys. C.

[10] ALEPH Collaboration, *Performance of the ALEPH Detector at LEP*, N.I.M. A360 (1995) 481

[11] ALEPH Collaboration, *Measurement of the Fraction of Hadronic Z Decays into Charm Quark Pairs*, CERN-EP/98-035, to appear in Eur. Phys. J. C.

[12] ALEPH Collaboration, *A Measurement of* R_b *using a Lifetime-Mass Tag*, CERN–PPE/97-017, Phys. Lett. **B401**, (1997) 150,
A Measurement of R_b *using Mutually Exclusive Tag*, CERN–PPE/97-018, Phys. Lett. **B401**, (1997) 163

[13] A. Falk and M. Peskin, Phys. Rev **D49**, (1994) 3320

[14] F. Becattini, in Proceedings of the 'Strangeness and Quark Matter 97' conference (Santorini), hep-ph/9708248 (1997)

[15] Yi-Jin pei, Z. Phys. **C72**, (1996) 39

[16] CLEO Collaboration (J. Gronberg et al.), CLNS(97/1501) (1997)

[17] ALEPH Collaboration, *Production of Orbitally Excited Charm Mesons in Semileptonic B Decays* , Z. Phys. **C73**, (1997) 601

[18] V Morénas et al., Phys. Rev. D **56**, (1997) 5680

[19] A. K. Leibovich et al., Phys. Rev. Lett. **78**, (1997) 3995

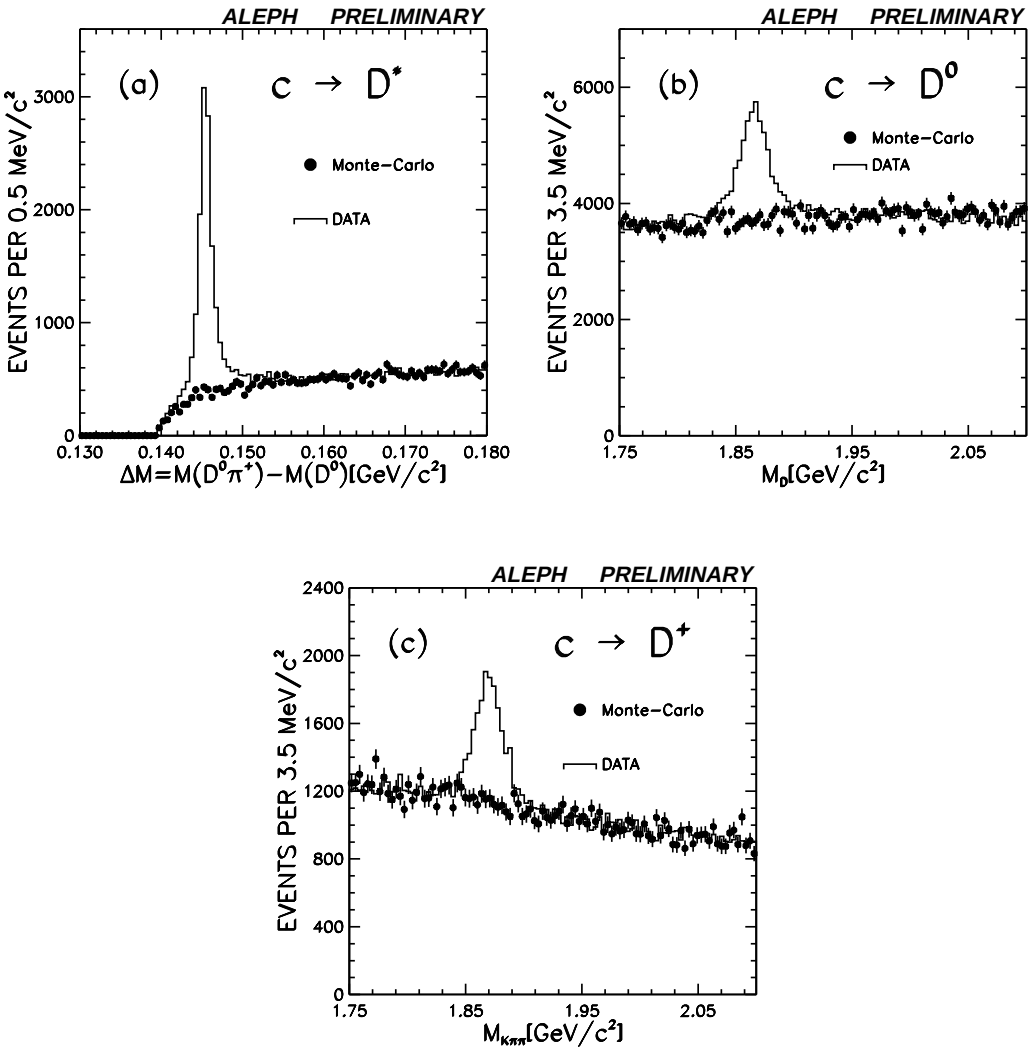

Figure 1: *Charm sample: (a) Mass difference distributions* $\Delta M \equiv M(\pi_s^+ \mathrm{D}^0) - M(\mathrm{D}^0)$ *for candidates of the decay channel* $\mathrm{c} \rightarrow \mathrm{D}^{*+} \rightarrow \mathrm{D}^0 \pi_s^+$ *followed by* $\mathrm{D}^0 \rightarrow \mathrm{K}^-\pi^+$, $\mathrm{D}^0 \rightarrow \mathrm{K}^-\pi^+\pi^0$ *and* $\mathrm{D}^0 \rightarrow \mathrm{K}^-\pi^+\pi^+\pi^-$. *(b) (c) Mass distributions for candidates of the decay channel* $\mathrm{c} \rightarrow \mathrm{D}^0, \mathrm{D}^0 \rightarrow \mathrm{K}^-\pi^+, \mathrm{D}^0 \rightarrow \mathrm{K}^-\pi^+\pi^+\pi^-$ *(b) and* $\mathrm{c} \rightarrow \mathrm{D}^+, \mathrm{D}^+ \rightarrow \mathrm{K}^-\pi^+\pi+$ *(c). The full histogram are the data while the dots with error bars are the combinatorial background taken from Monte Carlo simulation.*

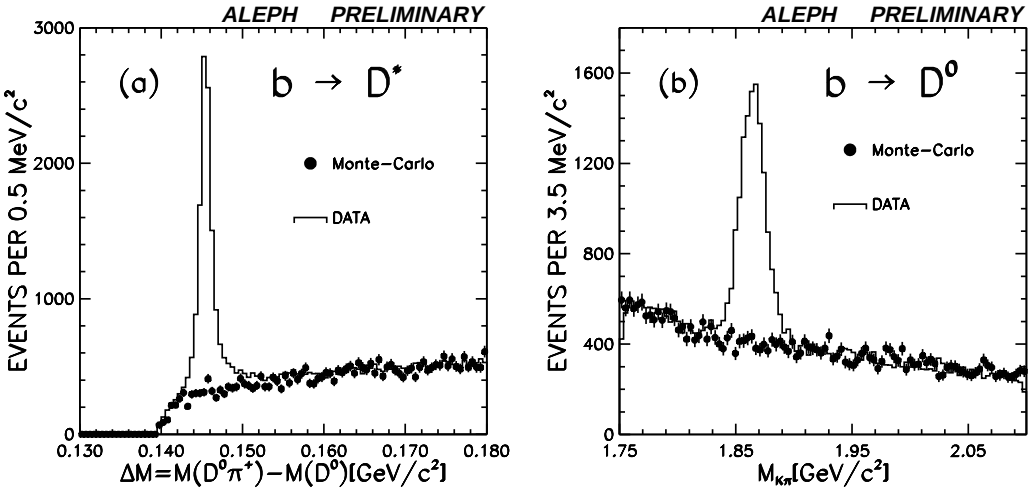

Figure 2: *b sample: (a) Mass difference distributions* $\Delta M \equiv M(\pi_s^+ \mathrm{D}^0) - M(\mathrm{D}^0)$ *for candidates of the decay channel* $\mathrm{c} \rightarrow \mathrm{D}^{*+} \rightarrow \mathrm{D}^0\pi_s^+$ *followed by* $\mathrm{D}^0 \rightarrow \mathrm{K}^-\pi^+$, $\mathrm{D}^0 \rightarrow \mathrm{K}^-\pi^+\pi^0$ *and* $\mathrm{D}^0 \rightarrow \mathrm{K}^-\pi^+\pi^+\pi^-$. *(b) Mass distribution for candidates of the decay channel* $b \rightarrow \mathrm{D}^0, \mathrm{D}^0 \rightarrow \mathrm{K}^-\pi^+$. *The full histogram are the data while the dots with error bars are the combinatorial background taken from Monte Carlo simulation.*

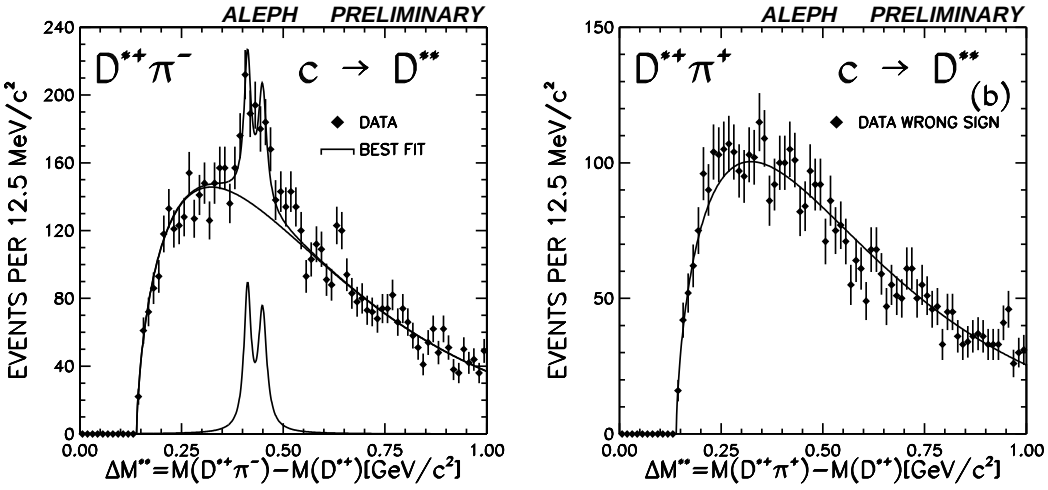

Figure 3: *Charm sample: Mass difference distributions* $\Delta M^{**} \equiv (\mathrm{D}^{*+}\pi^-) - \mathrm{D}^{*+}$ *in the decay channel* $\mathrm{c} \rightarrow \mathrm{D}^{**}$. *a) opposite sign combinations (* $\mathrm{D}^{*+}\pi^-$*). b) wrong sign combinations (* $\mathrm{D}^{*+}\pi^+$*). The solid line shows the result of the fit for the background function , together with the two Breit-Wigners in addition in figure (a).*

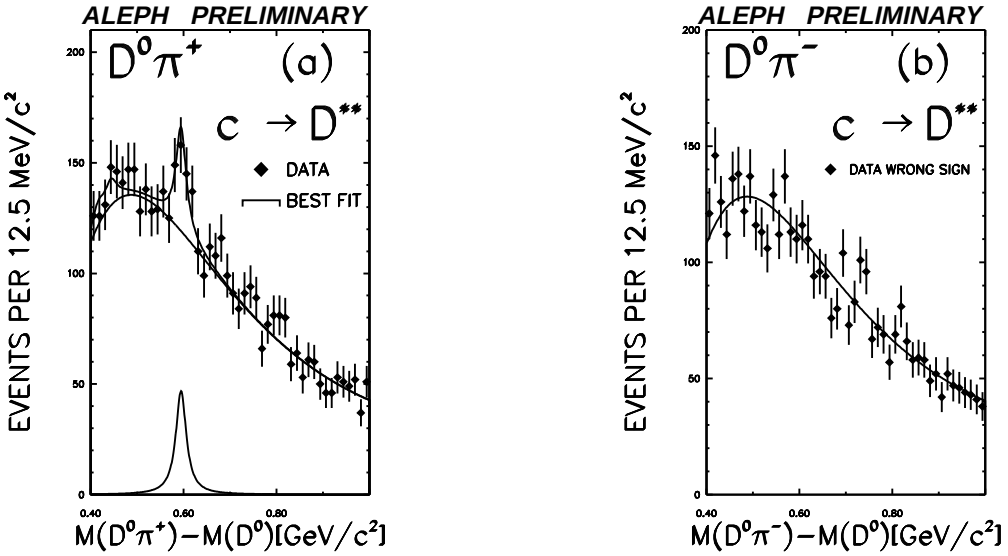

Figure 4: *Charm sample: Mass difference distributions* $\Delta M^{**} \equiv (\mathrm{D}^0\pi^+) - \mathrm{D}^0$ *in the decay channel* $\mathrm{c} \to \mathrm{D}^{**}$. *a) opposite sign combinations (* $\mathrm{D}^0\pi^+$*). b) wrong sign combinations (* $\mathrm{D}^0\pi^-$*). The solid line shows the result of the fit for the background function , together with the* D_2^* *Breit-Wigner in addition in figure (a).*

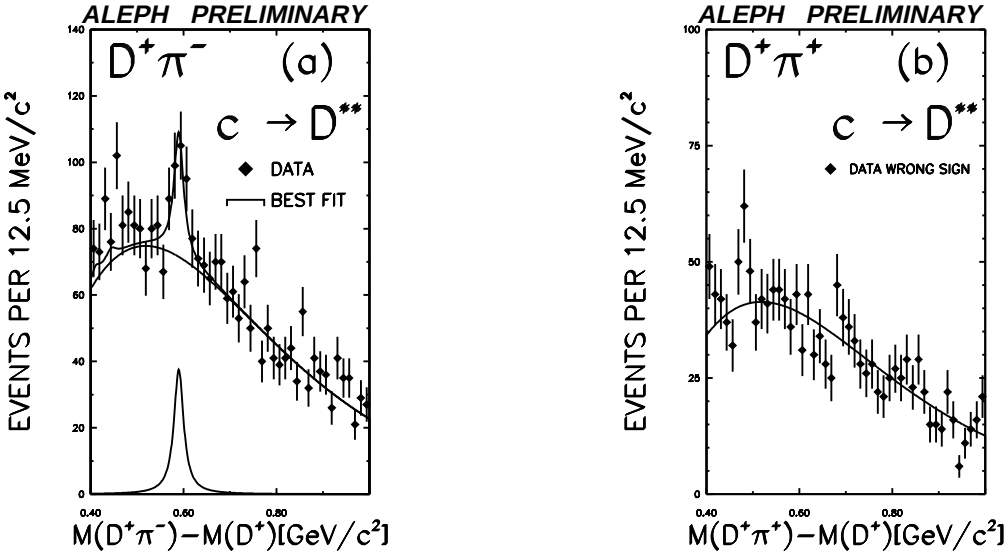

Figure 5: *Charm sample: Mass difference distributions* $\Delta M^{**} \equiv (\mathrm{D}^+\pi^-) - \mathrm{D}^+$ *in the decay channel* $\mathrm{c} \to \mathrm{D}^{**}$. *a) opposite sign combinations (* $\mathrm{D}^+\pi^-$*). b) wrong sign combinations (* $\mathrm{D}^+\pi^+$*). The solid line shows the result of the fit for the background function , together with the* D_2^* *Breit-Wigner in addition in figure (a).*

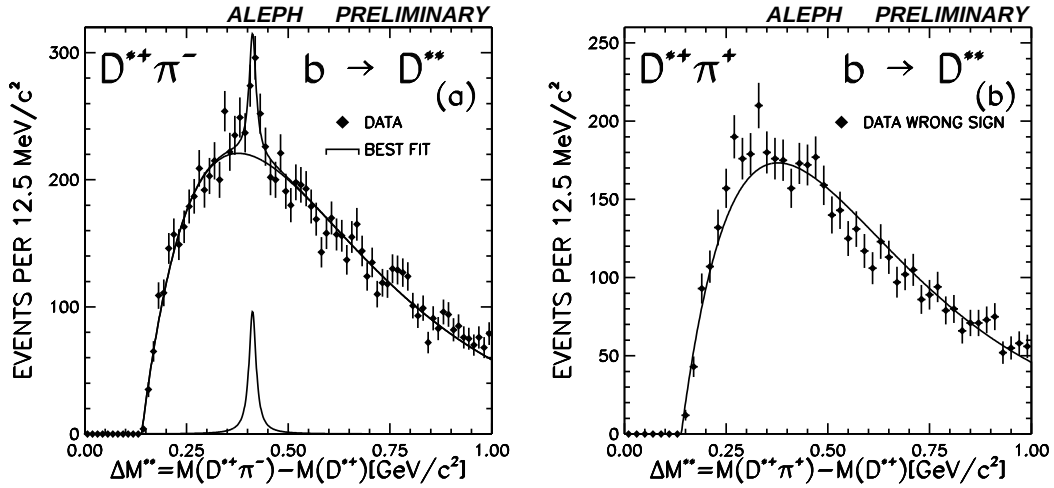

Figure 6: *b sample: Mass difference distributions* $\Delta M^{**} \equiv (\mathrm{D}^{*+}\pi^-) - \mathrm{D}^{*+}$ *in the decay channel* $\mathrm{b} \to \mathrm{D}^{**}$. *a) opposite sign combinations (* $\mathrm{D}^{*+}\pi^-$*). b) wrong sign combinations (* $\mathrm{D}^{*+}\pi^+$*). The solid line shows the result of the fit for the background function , together with the two Breit-Wigners in addition in figure (a).*

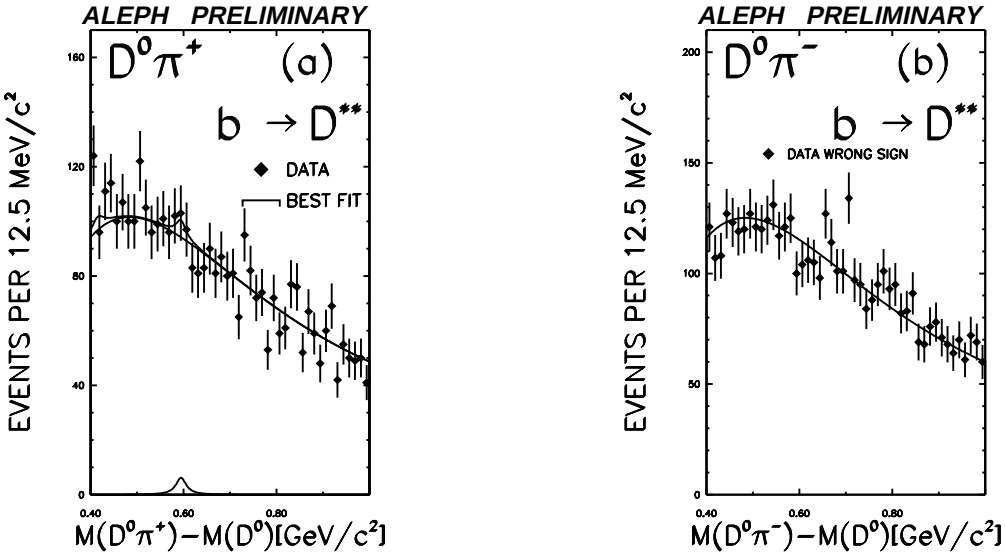

Figure 7: *b sample: Mass difference distributions* $\Delta M^{**} \equiv (\mathrm{D}^0\pi^+) - \mathrm{D}^0$
in the decay channel $\mathrm{b} \to \mathrm{D}^{**}$. *a) opposite sign combinations (* $\mathrm{D}^0\pi^+$*). b) wrong sign combinations (* $\mathrm{D}^0\pi^-$*). The solid line shows the result of the fit for the background function , together with the* D_2^* *Breit-Wigner in addition in figure (a).*